Journal of Inclusion Phenomena and Macrocyclic Chemistry **46:** 187–193, 2003.

Intercalation and Electrochemical Studies of Nitroprusside Anion into Zn-Al Layered Double Hydroxide

LUIZ FERNANDO DA SILVA, JAIRO TRONTO, HERENILTON PAULINO OLIVEIRA and JOÃO BARROS VALIM*

Departamento de Química, Faculdade de Filosofia Ciências e Letras de Ribeirão Preto, Universidade de São Paulo; Av. Bandeirantes 3900, Ribeirão Preto, Brasil, 14.040-901

(Received: 10 December 2002; in final form: 12 June 2003)

Key words: anionic clays, hydrotalcite-like compounds, intercalation, layered double hydroxides, nitroprusside anions

Abstract

The aim of the present work was to investigate the synthesis, characterization and electrochemical properties of the nitroprusside anions (NP) into zinc and aluminium layered double hydroxides (LDHs). The materials were prepared by the coprecipitation method under constant pH, followed by a hydrothermal treatment. The prepared materials were characterised by a set of analysis methods, such as powder X-ray diffraction (PXRD), Fourier transform infrared spectroscopy (FT-IR), thermogravimetry (TG), scanning electron microscopy (SEM) and cyclic voltammetry (CV). The results showed that the electrochemical response of NP ions into LDH structure is similar to that found for complex ions free in solution. In addition, our results reveal the dependence of the electrochemical response on the nature of the supporting electrolyte, for either cationic or anionic species.

Introduction

Layered double hydroxides (LDH), also known as hydrotalcite-like compounds, belong to a class of lamellar compounds that enables the incorporation of several species by guest-host chemistry [1]. LDHs structure can be described by considering the brucite-like structure, $Mg(OH)_2$, in which the Mg(II) cations are in the center of edge-sharing octahedra, with hydroxyl groups in their vertices, resulting in a planar structure. When some of the divalent cations in this structure are isomorphously replaced by trivalent ones, the layers become positively charged and in order to balance this positive charge, anions must be intercalated between the layers along with water molecules, resulting in the hydrotalcite-like structure [2, 3]. The chemical composition of this class of intercalation compounds can be expressed by the general formula $[M^{2+}_{1-x}M^{3+}_{x}(OH)_2]A^{m-}_{x/m}\cdot nH_2O$: where M^{2+} and M^{3+} are respectively the divalent and trivalent cations in the brucite-like layers and A^{m-} is the charge-balancing interlayer anion. The specific charge of the layer is directly related to the exchange ratio [x in the general formula, $x = M^3/(M^{2+} + M^{3+})$]. Thus, a wide variety of LDHs can be obtained by varying the M^{2+} and M^{3+} cations species and their ratio, as well as the intercalated anion A^{m-}, which can be exchanged by an ion-exchange process. Due to their properties, several new LDHs compounds have been prepared with potential technological applications, such as heterogeneous catalysis, host structures for photoactivation and photocatalysis and ion exchange [2, 3]. Among other applications, LDHs can also be used as modifiers of electrode surfaces. This interest arose from their smooth flexible structure with relatively low interlayer bonding, thermal and chemical stability, surface properties, as well as the low cost of their synthesis. Several reports have shown the electrode preparation using the approach to confine electroactive species into synthetic hydrotalcite-like structure: in particular, studies involving metalloporphyrins, polyoxometalate anions and electroactive anionic species ($[Fe(CN)_6]^{3-}$ and $[Ru(CN)_6]^{4-}$) [4–9]. Taking advantage of these properties, the goal of the present work was to investigate the electrochemical properties of pentacyanonitrosylferrate(II) ion, $[Fe(CN)_5NO]^{2-}$ nitroprusside ion (NP), into a confined medium. This anion was chosen due to its photochemical properties, reactivity and also because it plays an important role in physiological processes (peripheral vasodilator in hypertensive crises and cardiac failure) [10–15]. These physiological actions are due to the one-electron reduction of $[Fe(CN)_5NO]^{2-}$ to $[Fe(CN)_5NO]^{3-}$ which releases the nitric oxide after the dissociation of the Fe—NO bond [13–14]. In spite of the well-known nitroprusside's biological effects, the nature of the overall electrochemical processes involved in this field is still a matter of discussion [16–18]. The matter for the controversy of these studies is the nature of the product of one-electron reduction of nitroprusside ion as well as the mechanism of its formation. So, in the present paper, we report the synthesis, characterization and the electrochemical properties of nitroprusside anion intercalated into Zn-Al layered double hydroxides (ZnAl-NP-LDHs).

* Author for correspondence. E-mail: jobarval@ffclrp.usp.br

Experimental

Materials

All reagents used are of analytical grade and were supplied by Mallinckrodt® and no previous purification was carried out. All water used was distilled and further purified using a Millipore MilliQ® system.

Synthesis of the complex intercalated LDH

ZnAl-NP-LDHs were prepared using the constant pH coprecipitation technique. A solution containing 0.250 mol of $Zn(NO_3)_2$ and 0.125 mol of $Al(NO_3)_3$ in 260 cm^3 of water was added into a solution containing 0.0333/m (where m is the anion total charge of nitroprusside anions) mol of the anion in 1.050 cm^3 of water. During this addition, a 2 mol dm^{-3} NaOH solution was also added into the reaction mixture, in order to keep the pH constant at 10.0 (±0.5 units). The solid product was separated and washed by centrifugation. A portion of the material was dried under vacuum in the presence of activated silica gel, at room temperature. The other portion was suspended in the anion solution at the same initial concentration, at pH = 8.00 (±0.2 units), and submitted to hydrothermal treatment at 70 °C during 24 hours. After the hydrothermal treatment, the obtained material was separated, washed, and dried as described above.

Characterisation

The powder X-ray diffraction patterns (PXRD) for the solid materials were obtained using Siemens D5005 equipment with a graphite monochromator selecting the $Cu_{K\alpha}$ radiation ($\lambda = 1.540$ Å). A step of $0.02°s^{-1}$ was used in the continuous method in a 2θ range 2–70°. Fourier transform infrared spectra (FT-IR) were acquired over the range 4450–450 cm^{-1} with 60 scans per sample in a Nicolet 5ZDX instrument, using pressed KBr pellets containing 2% of the sample. Thermogravimetric analyses (TGA) were performed with a TA Instruments SDT 2960 equipment, under a flux of 100 cm^3 min^{-1} of synthetic air, from room temperature to 1000 °C at heating rate of 10 °C min^{-1}. The morphology of the powder LDHs was analyzed by scanning electron microscopy (SEM) in a Zeiss DSM 960 – Digital Scanning Microscope. The C, N, H contents were determined using a Perkin-Elmer 2400 CHN instrument. Electrochemical experiments were performed using an EG&G Princeton Applied Research model 273 potentiostat interfaced to a personal computer using M270 software.

The conventional three-electrode arrangement was used, consisting of a glassy carbon working electrode, a platinum wire auxiliary electrode, and a reference electrode of saturated calomel reference electrode (SCE). The experiments were carried out in an inert atmosphere by bubbling N_2 through the solution at room temperature (24 °C) prior to the measurements. The LDHs films were formed by dropping 2 μL of a suspension of the LDH onto the glassy electrode and allowing the solvent to evaporate at room temperature. The glassy electrode was previously polished with an aqueous suspension of 0.05 μm alumina and then ultrasonically cleaned, rinsed with purified water, and dried at room temperature (24 °C).

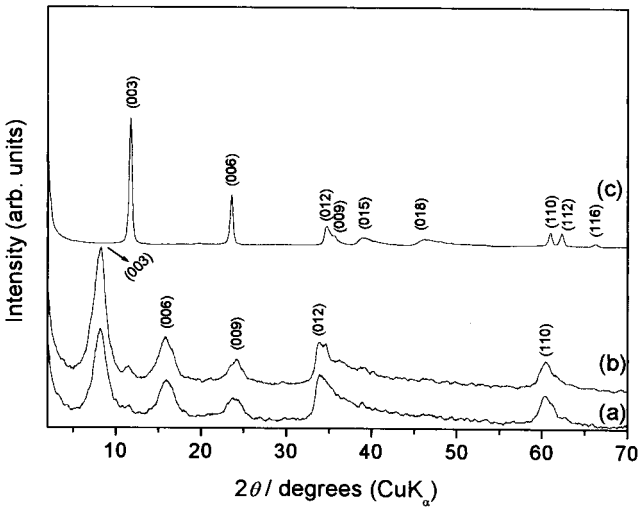

Figure 1. PXRD patterns for: ZnAl-NP-LDHs without hydrothermal treatment (a); ZnAl-NP-LDHs with hydrothermal treatment (b); ZnAl-CO_3-LDH (c).

Results and discussion

Powder X-ray diffraction

The PXRD patterns for the obtained materials are illustrated in Figure 1. A basal spacing of ~11.0 Å was obtained from the PXRD patterns for both ZnAl-NP-LDHs prior to and after the hydrothermal treatment. The values of basal spacing were calculated by the Bragg equation from (*00l*) peaks using the average $1/3(d_{003} + d_{006} + d_{009})$. The basal spacing values obtained are consistent with the size of nitroprusside anions, clearly indicating the intercalation of the complex [19]. By comparing the patterns of the materials obtained before and after the hydrothermal treatment (Figures 1a and 1b), we can observe that an improvement in the structural organization was achieved by this treatment. This higher crystallinity may be attributed to the self-organization of the NP anions in the interlamellar domain. The low-intensity diffraction peak, corresponding to a planar distance of approximately 7.6 Å, can be assigned to the presence of a very small amount of carbonate (contaminant from atmosphere) intercalated LDH. Molecular modelling calculations (Computational Program Spartan 5.0.2 with optimized geometry for the method PM3 tm) indicate that intercalated nitroprusside anions could be oriented in the position showed in Figure 2.

Fourier-transform infrared

FT-IR spectra of both ZnAl-NP-LDHs, prepared with and without hydrothermal treatment at 65 °C, and ZnAl-CO_3-LDH are shown in Figure 3. The broad band around

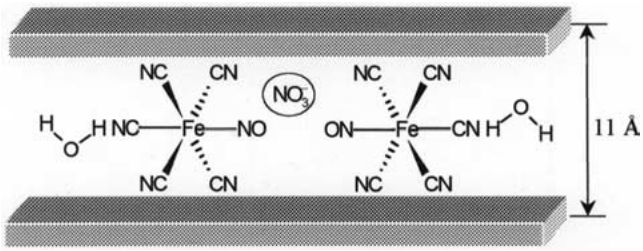

Figure 2. Proposed model for the structure of ZnAl-NP-LDHs.

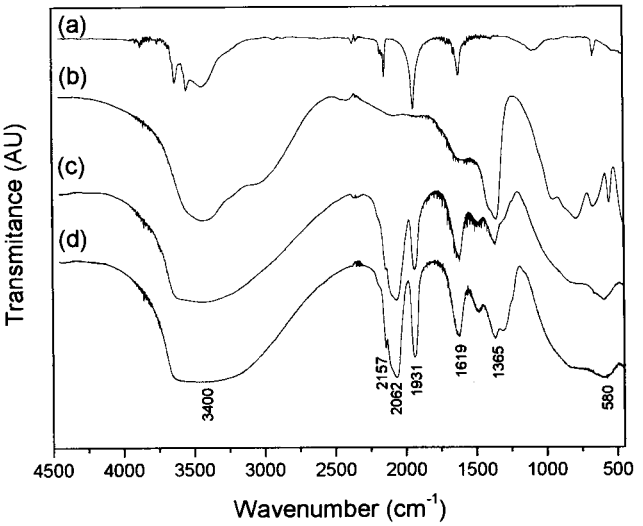

Figure 3. FTIR spectra of the nitroprusside ion (a); ZnAl-CO_3-LDH (b); ZnAl-NP-LDHs without (c) and with hydrothermal treatment (d).

3400 cm^{-1}, in the intercalated compounds spectra (Figures 3c and 3d), may be attributed to the stretching vibrations of the OH groups in the brucite-like layer and the peaks around 1365 cm^{-1} are related to ν_3 band of carbonate. The bands at 2157 cm^{-1} and 2062 cm^{-1} are related to CN stretching and the band at 1931 cm^{-1} is assigned to NO stretching. In addition, the composite band at 1619 cm^{-1} can be related to NO and OH stretching. Moreover, the peak at 580 cm^{-1} is assigned to Fe(II)-CN bending [18, 20, 21]. It is important to note that the intensity ratio between the bands due to NO and CN stretching observed for the intercalated compounds is smaller than that observed for pure sodium nitroprusside. This fact suggests a partial release of the nitric oxide ligand from the complex during the intercalation. According to literature [21], the presence of a new strong band at 2062 cm^{-1} in the intercalated materials, is due to the substitution of NO ligand by water molecule forming $[Fe(CN)_5H_2O]^{3-}$. This fact reinforces the hypothesis of the releasing of the nitric oxide. Thus, the coexistence of both $[Fe(CN)_5NO]^{2-}$ and $[Fe(CN)_5H_2O]^{3-}$ into interlamellar domain of ZnAl-LDH is possible.

Chemical analysis

Chemical analysis of carbon, nitrogen, and hydrogen, as well as the carbon/nitrogen ratio and Zn^{2+} and Al^{3+} contents are presented in Table 1. The $Zn^{2+}:Al^{3+}$ ratio added during the synthesis was 3 : 1. However, the analysis showed a reduced ratio of 2.68 : 1 for the material without hydrothermal treatment and 2.75 : 1 for the material after hydrothermal treatment. These differences can be explained by the solubilization of the Al^{3+} in the form of anion $Al(OH)_4^-$. The theoretical values of the C : N ratio for the nitroprusside anion is 0.83. The values for the LDHs are shown in Table 1. Supposing that practically every carbon atom is derived from nitroprusside anions (despising the contamination of the carbonate anions), the expected C : N ratio was 5 : 6. However, the results of chemical analyses showed that the ratio C : N was approximately 5 : 7. The decrease in this ratio is probably due to the presence of nitrate anions from precursor reagents used in the synthesis, which implies that the $NP^{2-}:NO_3^-$ ratio in the final sample is approximately 1 : 1.

Table 1. Elemental analysis of the ZnAl-NP-LDH

Sample	Hydr. treat.	C (%)	H (%)	N (%)	C : N	Zn : Al
1	Before	6.31	2.77	8.50	0.74	2.75
2	After	5.70	2.37	7.56	0.75	2.68

The approximate empirical formula calculated using the values in Table 1 and results of thermogravimetric analysis (next section) are $Zn_{2.7}Al(OH)_{7.6}(NP)_{0.25}(NO_3)_{0.5}\cdot 4.0H_2O$ for the material without hydrothermal treatment and $Zn_{2.8}Al(OH)_{7.4}(NP)_{0.25}(NO_3)_{0.5}\cdot 4.3H_2O$ for the material after hydrothermal treatment.

Thermogravimetric analysis

Thermogravimetric curves of ZnAl-NP-LDHs compounds with and without hydrothermal treatment are shown in Figure 4. Both materials present three steps of thermal decomposition. The first one, from the room temperature to 200 °C, corresponds to the release of adsorbed and interlamelar water molecules. The mass loss in this region was 14.1% (7.82×10^{-3} mol g^{-1}) for the material without hydrothermal treatment, and 15.0% (8.32×10^{-3} mol g^{-1}) for the material with hydrothermal treatment. The second step of decomposition was the loss of hydroxyl ions. For the ZnAl-NP-LDH without hydrothermal treatment the range of temperature was from 200 to 295 °C, corresponding to a mass loss of 7.75%. For the material after the hydrothermal treatment the range of temperature was from 200 to 330 °C, given a mass loss of 9.38%. The last step is related to the decomposition of the intercalated anions and the formation of mixed oxides. For the ZnAl-NP-LDH without hydrothermal treatment, the range of temperature was from 295 to 791 °C, with a mass loss of 11.6%. For the ZnAl-NP-LDH with hydrothermal treatment the range of temperature was from 330 to 785 °C, corresponding to a mass loss of 11.7%.

Scanning electron microscopy

SEM images of both the ZnAl-NP-LDHs samples prepared with and without hydrothermal treatment are shown in Figure 5. The SEM images for the materials, before and after the hydrothermal treatment, do not show a remarkable change

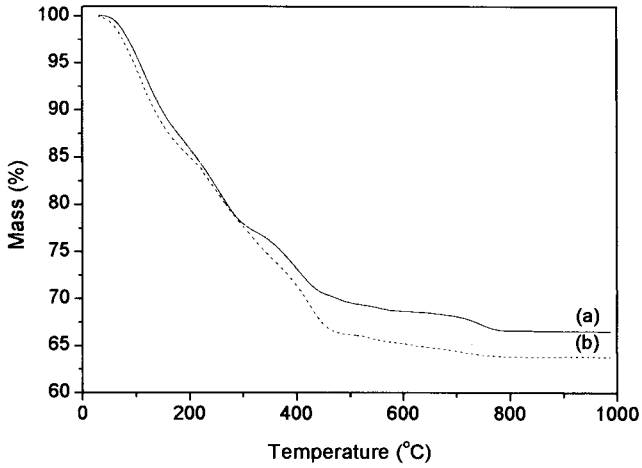

Figure 4. Thermogravimetric curves for the ZnAl-NP-LDHs without hydrothermal treatment (a) and after the hydrothermal treatment (b).

Table 2. Voltammetric parameters for a ZnAl-NP-LDH modified electrode concerning first one-electron reduction

Electrolyte	Epc/mV	Epa/mV	ΔE/mV
NaAc	−496	−211	285
NaCl	−458	−218	240
$NaClO_4$	−425	−198	227
$NaNO_3$	−410	−197	213
$KClO_4$	−448	−203	245
$NaClO_4$	−425	−198	227
$LiClO_4$	−387	−211	176

in morphology except for the fact that the hydrothermally treated material seems to be better stacked, which is in agreement with the increase of crystallinity of the sample after the hydrothermal treatment.

Cyclic voltammetry

Electrochemistry of the anionic complex

Electrochemical properties of the nitroprusside ion are still a matter of controversy, mainly concerning the nature of the one-electron reduction product, the redox mechanism, and the disproportionation/comproportionation processes [17].

Table 3. Voltammetric parameters for a ZnAl-NP-LDH modified electrode concerning second one-electron reduction

Electrolyte	Epc/mV	Epa/mV	ΔE/mV
NaAc	−695	−536	159
NaCl	−649	−482	167
$NaClO_4$	−630	−475	155
$NaNO_3$	−596	−468	128
$KclO_4$	−642	−510	132
$NaClO_4$	−630	−475	155
$LiClO_4$	−557	−505	52

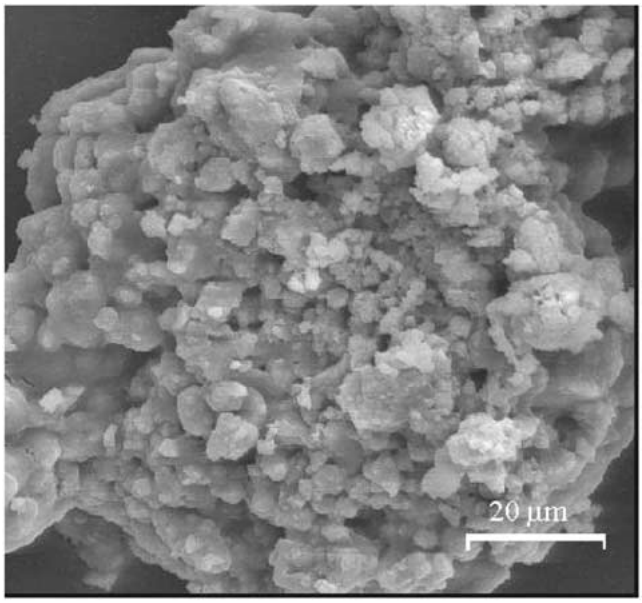

(A)

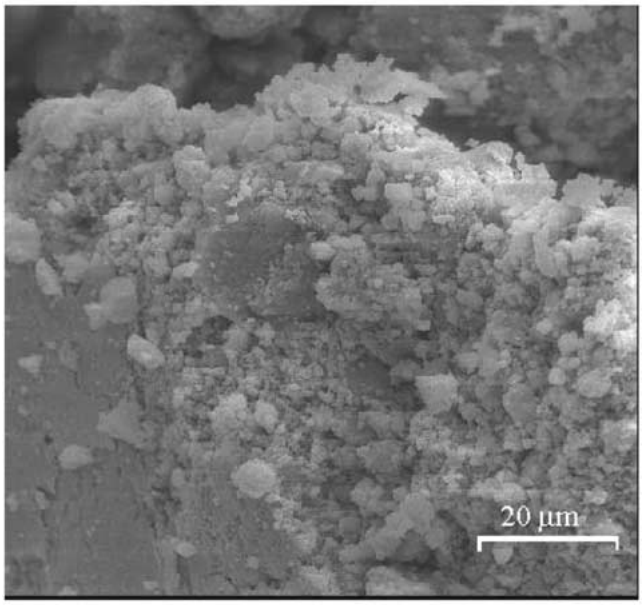

(B)

Figure 5. Scanning electron micrographs of the ZnAl-NP-LDHs without hydrothermal treatment (a) and after the hydrothermal treatment (b).

Based on electrochemical and spectroscopic studies, some authors support the formulation that after the first reduction process the formation of $[Fe(CN)_4NO]^{2-}$ occurs with the release of CN^-. In acid medium, this is the only reactant of second redox process because it favours the production of HCN. On the other hand, some authors state that after the one-electron reduction, the protonation of $[Fe(CN)_5NO]^{3-}$ occurs forming $[Fe(CN)_5NOH]^{2-}$, which is the only reactant of second redox process in acid medium [17]. Recently,

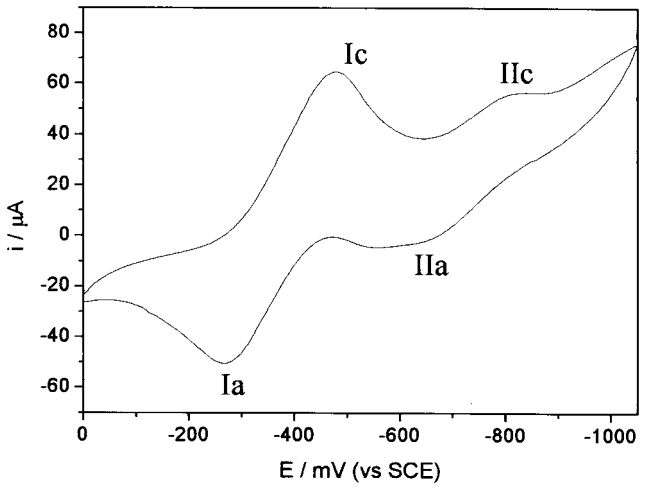

Figure 6. Cyclic voltammogram of nitroprusside ion in aqueous solution.

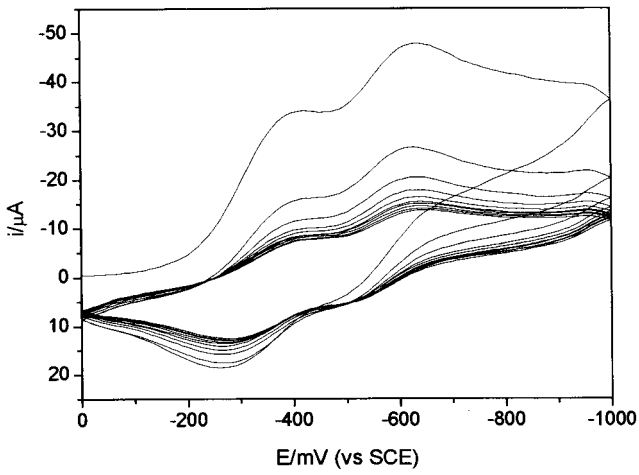

Figure 8. Stability essay of the ZnAl-NP-LDH in 0.5 mol dm^{-3} NaCl aqueous solution in the potential range 0.0 V to −1.0 V (*vs.* SCE) and $\nu = 100$ mV/s.

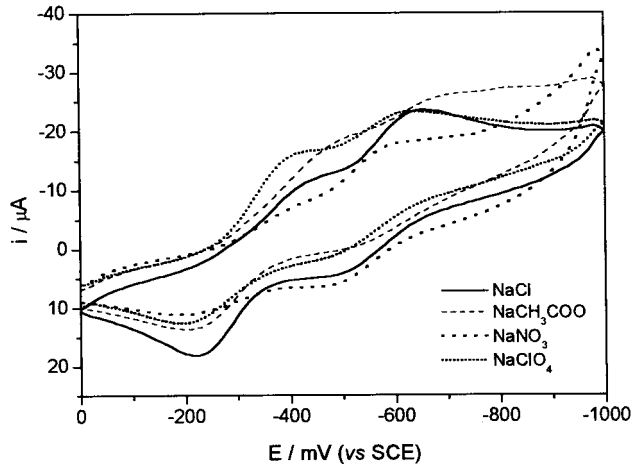

(a)

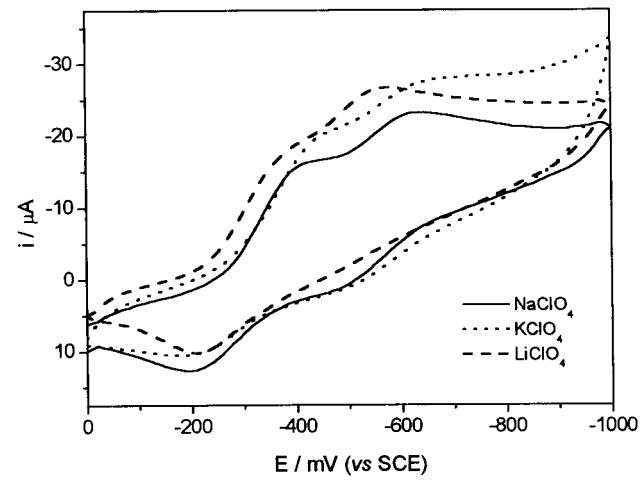

(b)

Figure 7. Cyclic voltammogram the ZnAl-NP-LDHs after the hydrothermal treatment obtained in different support electrolyte solutions: (a) anion as counter-ion; and (b) cation as counter-ion.

Lebrero and co-workers investigated the reduction products of nitroprusside ion using the density functional theory approach [18]. They found that for the first reduction product, $[Fe(CN)_5NO]^{3-}$, the optimisation and spectroscopic predictions were consistent with experimental results. In addition, $[Fe(CN)_5NO]^{3-}$ ions afford protonation on cyanide ligand. In order to clarify the previous information, an example of cyclic voltammogram of nitroprusside ion in aqueous medium is presented in Figure 6. Two pairs of peaks are observed on the voltammogram in the potential range from 0.00 V to −1.10 V (SCE). The redox peaks assigned Ipc/Ipa (between −0.50 V and −0.20 V) can be attributed to one-electron transfer ($[Fe(CN)_5NO]^{2-} + e \leftrightarrows [Fe(CN)_5NO]^{3-}$). The peaks IIpc/IIpa (between −1.20 V and −0.55 V) can be related to $(Fe(CN)_4NO]^{2-} + e \leftrightarrows [Fe(CN)_4NO]^{3-}$). Note that in this formulation we are assuming that CN^- ligand is released after one-electron reduction [16, 17]. However, the formation of protonated species after one-electron reduction ($[Fe(CN)_5NO]^{3-} + H^+ \leftrightarrows [Fe(CN)_5NOH]^{2-}$) can not be ruled out. And, in this case, many evidences reported in the literature suggest the formation of $[Fe(CN)_5NOH]^{3-}$ as a two-electron reduction product.

Electrochemical response of the nitroprusside anion into ZnAl-LDH

ZnAl-NP-LDH modified electrodes prepared by the dropping method resulted in inhomogeneous thin films with good adherence to the support electrode. Cyclic voltammograms of these electrodes obtained in different support electrolyte solutions are shown in Figures 7a and 7b and the electrochemical parameters for the first and second redox processes are summarized in Tables 2 and 3, respectively. For all voltammograms, two pairs of broad non-well defined oxidation-reduction peaks were observed between the ranges −0.50 V and −0.20 V, and −0.70 V and −0.40 V. Despite the peaks' shape, these results confirm that nitroprusside anions are present in the ZnAl-LDH structure. In other words, the obtained cyclic voltammograms are very similar to that found for nitroprusside ions in aqueous

medium, as shown in Figure 6 and discussed above. As observed in Figure 7, potential peaks, current peak intensities, and width at half-maximum are dependent of cation and anion nature. At a first glance, comparing these voltammograms with one of the NP in solution, the reversibility of both redox processes becomes more difficult, i.e., an increase of ΔEp values occurred. Probably, this fact can be related to the lack of adequate electronic conduction within the LDH structure. For voltammograms obtained in different support electrolyte solutions, varying the anion species (Na^+ as counter-ion, shown in Figure 7a), differences in peak potential values (ΔEp, in Table 4) were observed. The ΔEp values for process I changed from 285 mV in sodium acetate solution to 213 mV in sodium nitrate solution, and for process II there was a slight decrease of ΔEp values. So, it can be suggested that the anion effect is as follows: $Ac^- > Cl^- > ClO_4^- > NO_3^-$. Moreover, this variation in ΔEp values can be associated with the capacity of some anionic species to stabilize the lamellar structure of LDHs, which, according to Miyata's study, is in the order: $CO_3^- > OH^- > F^- > Cl^- > SO_4^{2-} > Br^- > NO_3^- > ClO_4^- > I^-$, and refers to kinetics of anionic substitution that depends on the size and geometry of the anion as well as their charge/radium relation [22]. Thus, probably an anionic exchange reaction occurs into lamellar domain and the electrochemical processes become irreversible when the medium contains anions that promote a higher stabilization of the structure. Another observation is that ohmic drop compensation and diffusion limitation inside the LDH should be considered in order to have a better interpretation of the electrolyte size effects, and these features are now under investigation in our laboratory. In addition, similar behavior was observed when cations species were changed. In solutions containing different cations (perchloride as counter-ion, as shown in Figure 7b), a reversible response was obtained mainly for lithium solution: ΔEp values for process I changed from 245 mV in $KClO_4$ solution to 176 mV in $LiClO_4$ solution while for process II there was a decrease from 132 mV to 52 mV.

These results reveal the dependence of the electrochemical response on the nature of the supporting electrolyte, for either the cationic or the anionic species. First, it is possible to suppose that an anion exchange reaction occurs between NP ions into LDH gallery with electrolyte anion from supporting solution. In this case, the system becomes reversible when the anionic specie forms a less stable LDH structure. So, the charge transport mechanism through the modifying layer implies that the electroactive specie undergoes ion exchange reaction with anions from the surroundings supporting electrolyte prior to the electron transfer [5, 23]. Second, the dependence on the electrolyte cation means that this specie can be sorbed or exchanged in order to maintain the charge neutrality. Finally, the electron transfer via electron-hopping can not be ruled out. In fact, it was noted that after few successive scans in the 0.0 V to 1.0 V (*vs.* SCE) potential range, the electrochemical response of ZnAl-NP-LDH modified electrode in NaCl supporting electrolyte solution becomes stable and retains its reversibility (Figure 8). These effects suggest that there are NP ions strongly bounded into LDH galleries and that these ions are not totally leached out of the lamellar structure [7]. Thus, this is an evidence that the electron transfer should occur via electron-hopping, accomplished with the incorporation of counter-anions to maintain the electroneutrality. Another possibility is the presence of some electroactive species located at the edge sites of the LDH micro-crystallites, near the support electrode, that contribute to an overall electrochemical response via the electron-hopping process [5, 7, 23].

Comparing the voltammograms of nitroprusside (II) anions into ZnAl-LDH, with another nitroprusside (II) in solution (Figure 6), an increase in the cathodic peak intensity for the second redox process in relation to the peak intensity of the first one can be verified for the ZnAl-NP-LDH. This suggests that the second cathodic process is favoured. This fact can be related to the release of cyanide ion. In other words, after the one-electron reduction of $[Fe(CN)_5NO]^{3-}$, the ion exchange reaction with electrolyte anion promotes the release of a cyanide anion [16, 17]:

$$[Fe(CN)_5NO]^{2-} + e \leftrightarrows [Fe(CN)_5NO]^{3-};$$

$$[Fe(CN)_5NO]^{3-} \leftrightarrows [Fe(CN)_4NO]^{2-} + CN^-.$$

This formulation is plausible because, with the first reduction process, the trans Fe—CN bond becomes weaker. This is probably due to the repulsion between the density of the added electron and the σ-bonding orbital from the donor CN^-. Thus, the release of the trans leaving group CN^- is favoured and, subsequently, the following reduction occurs [24]:

$$Fe(CN)_4NO]^{2-} + e \leftrightarrows [Fe(CN)_4NO]^{3-}.$$

Conclusion

In this paper we report the intercalation and characterisation of nitroprusside (NP) ion into a layered ZnAl-LDH, as well as its electrochemical behavior. Cyclic voltammetric studies revealed that the electrochemical response of NP ions into LDH structure is similar to that found for complex ions in solution. In addition, our results reveal the dependence of the electrochemical response on the nature of the supporting electrolyte, for either cationic or anionic species. The nature of charge transport through the modifying layer involves not only an extracrystalline mechanism (an ion exchange reaction between the electroactive anion complex with anions in the surrounding supporting electrolyte), but also that the redox process occurs via an intracrystalline mechanism through electron-hopping. In both possibilities, counter ions are incorporated into the LDH structure in order to maintain the electroneutrality of the system. Concerning the electrochemistry of NP ion in a confined medium, our experiments reveal that the two redox peaks are attributed to one-electron transfer ($[Fe(CN)_5NO]^{2-} + e \leftrightarrow [Fe(CN)_5NO]^{3-}$), followed

by the release of CN^- ligand and, subsequently, a reduction of $Fe(CN)_4NO]^{2-}$ to $[Fe(CN)_4NO]^{3-}$.

Acknowledgements

The authors are grateful to Dr. Sérgio Emanuel Galembeck for the computational calculations. This work was financially supported by Fundação de Amparo à Pesquisa do Estado de São Paulo – FAPESP (process 01/01527-5 and 02/00130-7), Coordenação de Aperfeiçoamento de Pessoal de Nível Superior – CAPES and Conselho Nacional de Desenvolvimento Científico e Tecnológico – CNPq.

References

1. F. Cavani, F. Trifiro and A. Vaccari: *Catal. Today* **11**, 173 (1991).
2. S.P. Newman and W. Jones: *New. J. Chem.* **22**, 105 (1998).
3. E.L. Crepaldi and J.B. Valim: *Quim. Nova* **21**, 300 (1998).
4. C. Mousty, S. Therias, C. Forano, and J.-P. Besse: *J. Electroanal. Chem.* **374**, 63 (1994).
5. S. Therias, C. Mousty, C. Forano, and J.-P. Besse: *Langmuir* **12**, 4914 (1996).
6. J. Qiu and G. Villemure: *J. Electroanal. Chem.* **428**, 165 (1997).
7. S. Therias, B. Lacroix, B. Schöllhorn, C. Mousty, and P. Palvadeau: *J. Electroanal. Chem.* **454**, 91 (1998).
8. A. Doménech, A. Ribera, A. Cervilla, and E. Lopis: *J. Electroanal. Chem.* **458**, 31 (1998).
9. K. Yao, M. Taniguchi, M. Nakata, and Yamagishi: *J. Electroanal. Chem.* **458**, 249 (1998).
10. G. Stochel: *Coord. Chem. Rev.* **114**, 269 (1992).
11. J.A . McCleverty: *Chem. Rev.* **79**, 53 (1979).
12. Z.-Z. Gu, O. Sato, T. Iyoda, K. Hashimoto, and A. Fujishma: *Chem. Mater.* **9**, 1092 (1997).
13. M.J. Clarke and J.B. Gaul: *Struct. Bond.* **81**, 147 (1993).
14. J. Oszajca, G. Stochel, E. Wasielewska, Z. Stasicka, R.J. Gryglewski *et al.*: *J. Inorg. Biochem.* **69**, 121 (1998).
15. A.H. Swirgiel, V.S. Palamarchouk, G. Smagin, and A.J. Dunn: *Brain Research Bulletin* **45**(2), 125 (1998).
16. C. Glidewell and I.L. Johnson: *Inorg. Chim. Acta* **132**, 145 (1987).
17. H.M. Carapuça, J.E.J. Simão and A.G. Fogg: *J. Electroanal. Chem.* **455**, 93 (1998).
18. M.C.G. Lebrero, D.A. Scherlis, G.L. Estiú, J.A. Olabe, and D.A. Estrin: *Inorg. Chem.* **40**, 4127 (2001).
19. J.W. Boclair, P.S. Braterman, B.D. Brister, and F. Yarberry: *Chem. Mater.* **11**, 2199 (1999).
20. R. Nast and J. Schmidt: *Angew. Chem. Internat. Edit.* **8**, 383 (1969).
21. S. Idemura, E. Suzuki, and Y. Ono: *Clays Clay Miner.* **37**, 553 (1989).
22. S. Myata: *Clays Clay Miner.* **31**, 305 (1983).
23. D.R. Rolison: *Chem. Rev.* **90**, 867 (1990).
24. R.P. Cheney, M.G. Simic, M.Z. Hoffman, I.A. Taub, and K.D. Asmus: *Inorg. Chem.* **16**(9), 2187 (1977).